# Comparative Evaluation of Fluorinated and Unfluorinated Acrylic Copolymers as Water-Repellent Coating Materials for Stone

G. ALESSANDRINI,[2] M. AGLIETTO,[1] V. CASTELVETRO,[1] F. CIARDELLI,[1] R. PERUZZI,[2] L. TONIOLO[2]

[1] Dipartimento di Chimica e Chimica Industriale, Via Risorgimento 35, 56126 Pisa, Italy

[2] Centro C.N.R. "Gino Bozza," Piazza Leonardo da Vinci 32, 20133 Milano, Italy

*Received 1 July 1999; accepted 14 September 1999*

**ABSTRACT:** An investigation on the influence of side-chain fluorination on the performance of a series of acrylic-based copolymers as protective coating materials for stones has been carried out by comparing them with unfluorinated polymeric analogues. For this purpose, a series of copolymers of 1H,1H,2H,2H-perfluorodecyl methacrylate (XFDM) and 2,2,2 trifluoroethyl methacrylate (TFEM) with unfluorinated vinyl ether or acrylic comonomers have been synthesized, as well as their not fluorinated analogues, and applied to limestone and marble substrates. A silicone-type commercial product, widely employed in the protection of stones in buildings and other artifacts, has also been tested as a reference material. Their protection efficiencies were then comparatively evaluated in terms of surface properties, water permeability, and appearance. It is shown that the presence of fluorine always has, as expected, a positive influence on the protective action of the polymer, increasing the water repellency of the coated stone.
 J Appl Polym Sci 76: 962–977, 2000

**Key words:** fluorinated polymers; acrylic copolymers; stone protection; water-repellent coating

## INTRODUCTION

Fluorinated polymers have gained growing popularity in the last years, with a renewed interest pushed from the scientific side by newly developed synthetic and application techniques,[1] and pulled from the industrial side by the increasing demand of high-performance, durable materials with unusual interfacial properties.

From the simplest fluorinated olefin homopolymer (PTFE) to the more recently developed highly engineered polymeric structures containing fluorinated vinyl ethers, urethanes, siloxanes, and acrylic units, partially fluorinated polymers have found wide application as coating materials with a number of interesting properties. They are increasingly employed and studied as antifouling,[2] water-repellent, low refractive index films, and in compositions for pressure-sensitive adhesives, self-lubricating surfaces,[3] thermally and chemically stable materials, among others. Partially fluorinated polymeric materials are finding increasing popularity even as components for high-performance paint and varnish formulations, in the textile, leather, and construction industry,[4] i.e., in application fields considered to be characterized by mature technology.

In the last few years poly(perfluoroalkyl ether)s and fluorinated elastomeric materials

*Correspondence to:* V. Castelvetro.
Contract grant sponsor: C.N.R. "Safeguard of Cultural Heritage" Target Project.

Journal of Applied Polymer Science, Vol. 76, 962–977 (2000)

have also been employed in the protection and consolidation of degraded surfaces of ancient buildings of great cultural importance.[5] Indeed, the deterioration and decay of natural stone buildings and manufacts is becoming a major concern, as the consequence of the often-observed acceleration of their degradation process and of the increasing interest in a conservationist approach to the symbols of our cultural heritage. Most ancient cathedrals and historic buildings, as well as valuable modern constructions and manufacts, are located in urban areas, and their condition has considerably worsened in this century, due to the synergistic action of natural weathering and high concentrations of air pollutants. Water penetration through the stone surface accounts for most of the deterioration processes occurring to the stone.[6–8]

Water is naturally present in variable amount within the porous structure of stone according to a thermodynamic equilibrium with the environmental humidity; however, the rainwater, which penetrates the stone by capillary absorption, is the vehicle of airborne acidic pollutants that exert a direct influence on the substrate, namely through the chemical reaction of dissolved $CO_2$, $NO_x$, and $SO_2$ with the calcareous substrates. Moreover, water exerts an indirect influence by changing the cohesion properties of the stone crystalline structure through a physical/mechanical decay due to thermal excursions in wet conditions (freeze–thaw cycles).

Although being very important, barrier efficacy against water penetration is not the only requirement for a protective coating material to be applied on the stone surfaces of cultural heritage buildings and sculptures.[9]

Italy has a particular interest in dealing with this issue, accounting for as much as 40% of the world cultural heritage (according to UNESCO). Therefore, the Italian "Normal" Committee (Committee for Stone Material Normalization) outlined the fundamental requirements that a protective coating material has to fulfill to be employed for such application;[10] these are, in addition to impermeability to liquid water, good permeability towards water vapor, chemical and photochemical stability, inertness towards the stone substrate (allowing reversibility of the treatment), and good optical properties (i.e., negligible short- and long-term modification of the appearance of the stone, in terms of color and gloss).

However, the scientific community is still far from the development of such an ideal material.[11] Until today, the most common approach of institutions and technicians involved in restoration and conservation research has been based on the use of materials either "traditional" or adopted from other application fields, without a previous indepth analysis of their advantages and disadvantages. In addition, the nature of the stone and its state of conservation, its geographical location, and its environmental exposure conditions are strongly variable; even the same stone type can be characterized by a very diverse behavior due to the intrinsic heterogeneity of the natural stone. Therefore, specific materials and application techniques are needed to satisfy the broad range of situations encountered in the field of restoration and conservation.

In the present article are presented the first results of a research, carried out in the framework of the C.N.R. (Italian National Research Council) "Target Project for the Safeguard of Cultural Heritage," aimed at designing, preparing, testing, and finally scale up the production of new partially fluorinated acrylic-based polymers as water-repellent stone coating materials.

The choice of the acrylic structure was suggested by the easily accessible and low-cost radical polymerization of the monomers, the availability of a broad range of monomers, and the possibility of tuning the material properties of the final polymers through appropriate design of the polymer structure and composition.[12] In addition, acrylic polymers are generally very suitable for coating purposes, and have been widely used in the field of conservation.[6] However, these materials proved to be a poor water repellent, and unstable to UV radiation on most stone substrates.[9,13] To overcome these disadvantages the synthesis of acrylic polymers with partially fluorinated side chains was carried out, and their increased water repellency, compared to that of not fluorinated analogues, was confirmed by preliminary studies.[14] These earlier results showed that an appropriate content and distribution of fluorine should be suitably combined with other functional groups in the macromolecular structure to allow a good anchorage onto the stone by means of the polar segments (e.g., the ester groups of the acrylic units), and that copolymers of fluorinated acrylic monomers with vinyl ethers can be characterized by interesting mechanical, thermal, and coating behavior.[15] More recent results have shown that even in the presence of fluorinated

comonomers, copolymers containing branched not fluorinated side chains, undergo rapid photodegradation with gel formation and crosslinking of the polymeric structure.[16]

Following this approach, in this article the assessment of the effectiveness of side-chain fluorinated acrylic-based copolymers as protective coatings on stone substrates is presented, in the framework of a systematic approach to the problem. The comparison between the performance of fluorinated and nonfluorinated polymeric analogues is described as a very useful way for the evaluation of the coating properties of these new materials. The influence of substitution of one of the methacrylic counits with the vinyl ether analogous (i.e., with the same alkoxy side chain) is also studied. The following fluorinated and unfluorinated monomers were employed: 1H,1H,2H,2H-perfluorodecyl methacrylate (XFDM), 2,2,2-trifluoroethyl methacrylate (TFEM), lauryl methacrylate (LM), methyl acrylate (MA), ethyl methacrylate (EM), and *n*-butyl vinyl ether (BVE); therefore, copolymers having different fluorine content and distribution along the macromolecular structure could be prepared.

Candoglia marble (Verbania, Italy) and Calcarenite of Noto (Siracusa, Italy), two carbonatic stone materials, were selected as the stone substrates for their very different porosimetric characteristics, and for their widespread use in ancient buildings of northern and southern Italy (e.g., in the Cathedral of Milan and in the baroque architecture of the small town of Noto, Sicily).

## EXPERIMENTAL

### Materials

Diethyl ether (Carlo Erba) was dried over $CaCl_2$, then distilled from $LiAlH_4$. Dioxane (C. Erba) was dried over $CaCl_2$, then distilled from Na. Toluene (C. Erba) was distilled from Na. Azobis-1,1-dimethyl-2-propionitrile ($\alpha,\alpha'$-azobis-isobutirronitrile, AIBN, Akzo) was purified by recrystallization from ethanol. Tetrahydrofuran (THF, spectroscopy grade, Fluka), ethyl acetate (spectroscopy grade, C. Erba), and petroleum ether (b.p. 160°C, C. Erba) were used as received. Triethylamine (Fluka) was distilled from $CaH_2$. The commercial coating materials Wacker 280™ (a liquid mixture of oligomeric alkylalkoxy siloxane with long and short alkyl groups and of silicic esters) and Acryloid B72™ (Rohm and Haas) were used as received. *n*-Butyl vinyl ether (BVE, Fluka) was distilled from Na/K alloy shortly before use. 2,2,2-Trifluoroethanol (Prosynth) and 1H,1H,2H,2H-perfluorodecan-1-ol (Strem Chemicals) were used as received. Methacryloyl chloride (Fluka) was distilled from quinoline, in the presence of di-*tert*-butyl-*p*-cresol (DTBC) as polymerization inhibitor. *n*-Dodecyl methacrylate (LM, lauryl methacrylate, Aldrich) was distilled at reduced pressure (110°C/0.2 mmHg) in the presence of DTBC. Methyl acrylate (MA, Aldrich) and ethyl methacrylate (EM, Aldrich) were added with DTBC and distilled under nitrogen. 2,2,2-Trifluoroethyl methacrylate (TFEM) and 1H,1H,2H,2H-perfluorodecyl methacrylate (XFDM) were synthesized from the fluorinated alcohol and methacryloyl chloride in the presence of triethylamine and a polymerization inhibitor, and purified either by distillation or by column chromatography, according to previously reported procedures.[17] All monomers were stored under nitrogen at −25°C before use.

#### *Poly(1H,1H,2H,2H-perfluorodecyl methacrylate-co-*lauryl methacrylate) (XFDM/LM)

In a 250-mL Schlenk tube were placed 2.73 g (5.1 mmol) of XFDM, 3.91 g (15.4 mmol) of LM, 0.11 g (0.72 mmol) of AIBN, and 36 mL of dry dioxane. The solution was degassed with three freeze–pump–thaw cycles and heated at 65°C under magnetic stirring for 76 h. The obtained product was precipitated in methanol, giving 9.15 g (65% yield) of XFDM/LM copolymer. Additional 1.30 g were recovered by precipitation from chloroform/hexane of the soluble fraction of the first precipitation (total yield 75%). IR: $\nu$ = 3000–2850, 1732, 1500–1360, 1350–1000 $cm^{-1}$. $^1$H-NMR: $\delta$ = 4.3–4.1 (XFDM, $OCH_2$), 4.1–3.7 (LM, $OCH_2$), 2.6–2.2 (XFDM, $CH_2CF_2$), 2.2–1.65 (main chain $CH_2$), 1.65–1.45 (LM, $OCH_2CH_2$), 1.45–1.2 (18H, LM, $(CH_2)_9CH_3$), 1.2–0.6 ($CH_3$) ppm.

#### *Poly(lauryl methacrylate) (PLM)*

LM (6.06 g, 23.8 mmol) and AIBN (0.15 g, 0.09 mmol) were dissolved in 43 mL of dry dioxane in a schlenk tube, degassed, and heated 70 h at 60°C. The product was then precipitated in methanol, yielding 5.16 g of dried polymer (90%). IR: $\nu$ = 2980–2800, 1732, 1500–1360, 1250–1100 $cm^{-1}$. $^1$H-NMR: = 4.1–3.7 ($OCH_2$), 2.1–1.7 (main chain $CH_2$), 1.7–1.45 ($OCH_2CH_2$), 1.45–1.2 ($(CH_2)_9CH_3$), 1.2–0.6 ($CH_3$) ppm.

#### *Poly(2,2,2-trifluoroethyl methacrylate-co-*methyl acrylate) (TFEM/MA)

TFEM (21.14 g, 125.8 mmol), MA (5.38 g, 62.5 mmol), and AIBN (0.92 g, 5.64 mmol) were dis-

solved in 200 mL of dry dioxane in a Schlenk tube, degassed, and heated at 60°C for 110 h under magnetic stirring. The product was then precipitated in methanol, yielding 25.7 g (97%) of TFEM/MA copolymer. IR: $\nu$ = 2960–2850, 1740, 1500–1360, 1350–1200 (C—F), 1200–1000 $cm^{-1}$. $^1$H-NMR: = 4.6–4.1 ($CH_2CF_3$), 3.7–3.4 ($OCH_3$), 2.6–2.0 (CHCOO), 2.1–1.2 (main chain $CH_2$), 1.4–0.6 (TFEM, 3H, $CH_3$) ppm.

### *Poly(2,2,2-trifluoroethyl methacrylate-co-butyl vinyl ether) (TFEM/BVE)*

Following the usual procedure, TFEM (10 g, 6.0 mmol), BVE (17.86 g, 0.18 mol), AIBN (0.39 g, 2.4 mmol), and 70 mL of dry dioxane were charged in a glass reactor, degassed, and heated at 70°C for 96 h under magnetic stirring. Precipitation from *n*-pentane gave 7.16 g of copolymer. The pentane filtrate was dried, and the resulting viscous oil was purified by silica gel chromatography, giving a further 3.28 g of copolymer that was added to the first fraction (38% total yield). IR: $\nu$ = 3000–2850, 1748, 1500–1375, 1350–1220 ($CF_3$), 1200–1000 $cm^{-1}$. $^1$H-NMR: = 4.6–4.1 ($OCH_2CF_3$), 3.4–2.9 (CH—O—$CH_2$), 2.2–1.4 (TFEM, $CH_3$; main chain $CH_2$), 1.7–1.1 ($CH_2CH_2CH_3$), 1.0–0.7 (BVE, $CH_3$) ppm.

### *Poly(ethyl methacrylate-co-*butyl vinyl ether) (EM/BVE)

Following the usual procedure, the two monomers (EM and BE) and AIBN were charged in a schlenk tube, degassed, and polymerized either in toluene or in bulk. The final product was recovered by precipitation in methanol. IR: $\nu$ = 2960–2800, 1748, 1200–1050 $cm^{-1}$. $^1$H-NMR: = 4.15–3,9 ($COOCH_2$), 3.7–2.9 (CH—O—$CH_2$), 2.1–1.6 (CHCOO), 1.6–0.6 (main chain $CH_2$).

## Techniques

$^1$H- and $^{13}$C-NMR analyses were recorded from $CDCl_3$ solutions on a Varian Gemini 200 spectrometer at 200 MHz. Chemical shifts were related to the $CHCl_3$ signal at 7.24 ppm vs. TMS. FTIR spectra were recorded from thin films cast on KBr pellets, using a Perkin-Elmer 1600 instrument. DSC analyses were carried out with a Perkin-Elmer DSC7 instrument equipped with a CCA7 temperature control apparatus connected with a liquid nitrogen tank; thermal analyses were performed at 20°C/min scan rate on the instrument calibrated with indium and mercury standards. Thermogravimetric analyses were carried out in nitrogen flux at 10°C/min from 25 to 600°C, using a Mettler TC11 TA processor connected with a Mettler TG 50 thermobalance. Size-Exclusion Chromatography (SEC) analyses were performed at room temperature on 50-$\mu$L samples (5 g/L polymer solutions in THF or chloroform) at 1 mL/min flux, on a Perkin-Elmer Model 2/2 instrument with a 150-$\mu$L sample loop, equipped with two PL GEL Mixed C columns (30 cm × 7.5 mm), a Jasco 830 RI differential refractometer, and a Perkin-Elmer LC-75 spectrophotometric detector. The molecular weight data are referred to a polystyrene standards calibration curve, and are not corrected; a further source of uncertainty in the molecular weight and MWD determination could be due to the observed nonlinear response of the RI detector to the partially fluorinated copolymers (the higher the F content, the lower the detector response, given the well-known low RI of fluorinated materials). As the consequence, a self-consistent MWD curve could have been obtained only if the copolymer composition had been the same, irrespective of the molecular weight of the single macromolecular chain. This is certainly not the case, as an unnegligible variability is to be expected, considering the fact that the copolymers were prepared in relatively high conversions and that monomers with very different reactivity were copolymerized, thereby producing a continuous change in the composition of the polymerizing mixture. Scanning electron microscopic observations on untreated and treated specimens were carried out with a JEOL JSM 35C microscope equipped with a LINK 10000 energy dispersive X-ray spectrometer.

Porosimetric measurements on representative stone samples (around 0.01 × 0.01 × 0.01 m) were performed using a Fisons 140/240 Hg Porosimeter; the stone samples were previously dried at 60°C for 24 h and stored in a dessiccator at room temperature before analysis.

## Stone Specimen Preparation and Characterization, Treatment Methodology, and Polymer Uptake

The calcarenite of Noto is a highly porous limestone, with around 30 vol % open-cell porosity, specific surface area of 1.6–2.0 $m^2/g$ and rather monodisperse pore radius average in the range of 4–10 $\mu$m, as determined by mercury porosimetry. The Candoglia marble is a highly crystalline, low-porosity stone with 0.5–0.7 vol % porosity, specific surface area of 0.01–0.03 $m^2/g$, and highly polydisperse

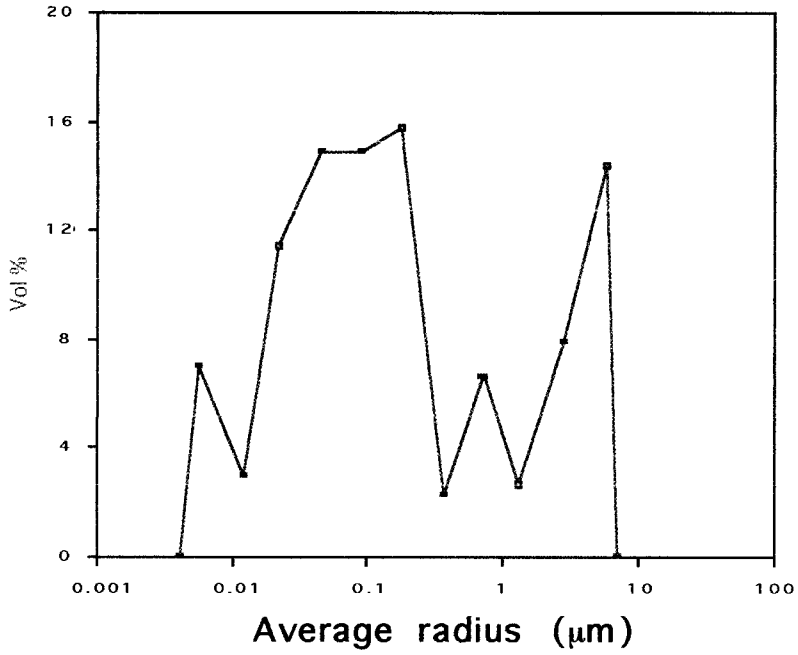


**Figure 1** Candoglia marble: pore size distribution.

pore radius distribution (Fig. 1). Twenty-five 5 × 5 × 1-cm stone specimens and 25 5 × 5 × 2-cm stone specimens were prepared both with the calcarenite of Noto and with the Candoglia marble. Each specimen surface was smoothed with abrasive carborundum paper (n.180). The specimens were then accurately washed with deionized water and dried 48 h at room temperature, 24 h at 40°C, and 24 h under vacuum (0.1 mmHg) at room temperature; they were finally weighed and stored in a dessiccator before treatment.

Application of the coating polymer solution was carried out by brush until refuse, or by capillarity absorption from a filter paper pad saturated with the polymer solution (6–7 h). The treatment methodology was suggested by the available amount of copolymer, because application by capillarity absorption on a lab scale requires comparatively larger volumes of polymer solution. After the treatment, the specimens were dried following the same procedure adopted for the conditioning of the untreated specimens. The stones treated with Wacker 280™ were kept for 2 months in a damp atmosphere (r.h. 80%), to allow the hydrolysis and to complete the polymerization and crosslinking, before carrying out the usual drying procedure. The amount of polymer deposited on the stone was determined by weighing (M ± 0.0001 g) each dried and conditioned specimen before and after treatment.

### Sessile Contact Angle Determination

Contact angle measurements were carried out, according to the relevant Normal protocol,[18] using a Lorentzen Wettre Surface Wettability Tester (modified by fitting it to a horizontally pivoted table). About 30 microdrops (3–5 μL) of deionized water were laid down with a syringe on different spots of the surface of each specimen, after application of the polymer coatings, and the contact angles were measured as:

$$\alpha = 2 \text{ arctg } 2\mathbf{h}/\mathbf{d}$$

where **d** is the drop base length, and **h** is the drop height. The resulting contact angle measurements were averaged for each stone specimen.

### Water Absorption by Capillarity

The determination was carried out using the gravimetric sorption technique, according to the Normal protocol,[19] on the 5 × 5 × 2 cm specimen. The stone specimen is laid on a filter paper pad around 1 cm thick, partially immersed in deionized water, with the treated surface in contact with the pad. The amount of water absorbed by capillarity forces is determined by weighing the specimen after 10′, 20′, 30′, and 1, 2, 4, 6, 24, 48, 72, and 96 h, to obtain the wet specimen mass $m_i$

(M ± 0.0001 g). The amount of absorbed water $M_i$, at the time $t_i$ per surface unit, is defined as follows:

$$M_i = (m_i - m_o)/S$$

where $m_i$ is the specimen mass (g) at the time $t_i$ (second) , $m_o$ is the dry specimen mass (g), and $S$ is the contact surface ($cm^2$). The $M_i$ values are plotted against the square root of time ($s^{1/2}$), according to the general adopted equation $Q = Kt^{1/2}$ $x$, where $Q$ is the amount of absorbed water, and $t$ is time (seconds),[20] to give the capillarity absorption curve.

### Water Vapor Permeability

The determination was carried out according to the corresponding Normal protocol[21] on the 5 × 5 × 1-cm specimen, using a measurement cell consisting in a cylindrical PVC chamber with open top fitted with an o-ring rubber seal, where the stone specimen is employed as the lid of the chamber, and the chamber is sealed with the lid by means of an aluminum flange with an o-ring. The cell is partially filled with deionized water, therefore allowing measurement by gravimetry the amount of water vapor that diffuses through the 0.01 m-thick stone specimen and through the central hole of the flange ($S = 0.00163$ $m^2$) to exit the cell. The test is carried out in a climatic chamber at constant temperature (20 ± 0.5°C), with the cell placed into a dessiccator. The driving force for the diffusion of water vapor is, therefore, the constant difference between the water vapor pressure inside (saturated water vapor pressure) and outside the cell (in the presence of activated silica gel desiccant). The permeability is monitored by determining the weight decrease per surface unit in the unit time (24 h):

$$\Delta M_i = (m_i - m_o)/S$$

The cell is weighed (M ± 0.0001 g) and $\Delta M_i$ (daily weight variation) is calculated when a stationary condition (constant vapor flow through the stone) is reached; stationary flow was considered to be reached when

$$(\Delta M_i - \Delta M_{i-1}) \times 100/\Delta M_i \leq 5\%$$

The permeability is evaluated before and after the treatment on the same specimen with the protective coating material.

### Colorimetric Analyses

The evaluation of color change on polymer-coated stones was carried out by means of a Minolta Chroma Meter colorimeter series CR200 in total reflectance and double channel mode, using a Xenon lamp light source; the determinations were carried out according to the corresponding Normal protocol[22] on the 5 × 5 × 2 and 5 × 5 × 1-cm specimens. The color changes were evaluated by the L*a*b* system (ASTM D-1925, CIE 1976), while the color characterization (wavelength $\lambda$ and excitation purity $P$) was determined by the Yxy system (CIE 1931).[23–25]

Twenty color determinations were carried out on different spots of each stone specimen before and after the treatment. The obtained data were elaborated to evaluate the effect, on the stone surface appearance, of the type of polymer and of the treating solution concentration. Due to the scattering of the obtained data, the significance of the observed variation was analyzed by the Student $t$ statistic test using the confidence level of 95%.

## RESULTS AND DISCUSSION

Two widely employed commercial products, namely the acrylic copolymer Acryloyd B72™ (essentially an EM/MA copolymer of 2 : 1 molar composition[26]) and the silicone Wacker 280™ were selected as reference materials for a comparative evaluation of the coating performance of the fluorinated acrylic-based copolymers. Although chemically different from all the other polymers, the silicone was chosen because of its good performance shown on both low- and high-porosity stones;[27] it should be noted, however, that although this latter product performs quite well, its mechanism of interaction with the stone is not reversible, as opposed to that of the acrylic copolymers. The average compositions and relevant MW and thermal characterization data of the synthesized acrylic polymers are reported in Table I. The copolymerization conditions were optimized to obtain copolymers with similar average molar composition, when comparing them within each "couple," that is, each partially fluorinated polymer with its unfluorinated analogous. Therefore, the difference observed in the material behavior within a polymer couple can be specifically ascribed to the replacement of H with F atoms, although additional minor contributions to varia-

**Table I Acrylic Polymers Employed**

| Polymer | Molar Composition[a] | $F$ (wt %) | $T_g$ (°C) | $M_n$ ($\times 10^{-4}$) | $M_w/M_n$ |
|---|---|---|---|---|---|
| XFDM/LM | 1/2.4 | 28.3 | −47/+5 | 6.6 | 1.1 |
| PLM | — | — | −47 | 1.5 | 2.6 |
| TFEM/MA | 2/1 | 27.0 | 43 | 2.1 | 1.7 |
| Acryloyd B72 | [b] | — | 43 | 1.7 | 3.7 |
| TFEM/BVE | 2.5/1 | 27.4 | 34 | 4.2 | 2.9 |
| EM/BVE | 2.5/1 | — | 26 | 9.8 | 1.2 |

[a] Determined by $^1$H-NMR.
[b] Essentially an EM/MA 2/1 copolymer.

tions in the coating performance could derive from differences in degree of polymerization (DP), molecular weight distribution (MWD), and such microstructural parameters as comonomer distribution and stereochemistry (tacticity).

In addition, the composition of the three fluorinated copolymers corresponds to a very similar overall fluorine weight content. Assuming that an average copolymer composition reflects a correspondingly average material behavior, that is, irrespective of any existing microstructure heterogeneity, the use of fluorinated copolymers with similar F content should allow to neglect the mass contribution of F to the protection efficiency of the coating, leaving as the main contribution the one deriving from the structure of the fluorinated comonomer. In this sense, copolymers of TFEM and XFDM are, in a way, antithetic to one another in terms of fluorine content and distribution, because a much higher mol fraction of the short side-chain TFEM is needed to obtain a copolymer with the same F content as a copolymer containing the highly fluorinated, long side-chain XFDM; therefore, the TFEM copolymer will have its short ($CF_3$) fluorinated groups distributed along the macromolecular chain with a much higher frequency compared to the case of the XFDM copolymer, with fewer but much longer ($nC_8F_{17}$) fluorinated moieties spaced apart along the chain (assuming a random comonomer distribution).

Several polymerization runs were carried out to obtain an EM/BVE copolymer with the desired composition and with acceptable yield, that is about the same molar composition (2.5 : 1) of the fluorinated TFEM/BVE analogous (see Table II).

The couples TFEM/MA–Acryloid B72™ and XFDM/LM– PLM were selected to evaluate the influence of partial side-chain fluorination on different copolymer structures, characterized by short and long side chains, respectively; the same comparison can be made between the "hybrid" copolymers TFEM/BVE and EM/BVE, where the unfluorinated (meth)acrylic comonomer is replaced by a vinyl ether.

A comparison between the TFEM/MA and the TFEM/BVE copolymers allows highlighting of the effect of substitution of an acrylate with a vinyl ether unit, the latter containing a relatively hydrophilic and less polar ether group and a longer, and therefore more hydrophobic, alkoxy chain. In addition, while all the fully acrylic copolymers can be expected to present an essentially random comonomer distribution, in the case of the BVE copolymer the poor tendency towards homopropagation of the vinyl ether under radical polymer-

**Table II Copolymerizations of EM with BVE[a]**

| EM (mol/L) | EM/BVE Feed (mol Ratio) | AIBN/EM (mol Ratio) | Conversion (wt %) | Copolymer Composition |
|---|---|---|---|---|
| 1.0 | 1/5 | 0.12 | 8 | 3.8/1 |
| 0.5 | 1/10 | 0.17 | 1 | n.d. |
| bulk | 1/10 | 0.02 | 2 | 2.5/1 |

[a] Solvent toluene, $T$ = 60°C, 72 h.

**Table III Polymer Solutions Applied on the Stone Specimens**

| Polymer Solution | Concentration (wt %)[a] | | Application Technique |
|---|---|---|---|
| XFDM/LM | 5 | 10 | brush |
| PLM | 5 | 10 | brush |
| TFEM/MA | 3 | 5 | capillarity |
| Acryloid B72 | 3 | 5 | capillarity |
| TFEM/BVE | 5 | 10 | brush |
| EM/BVE | 5 | 10 | brush |
| Wacker 280-C | 8[b] | | capillarity |
| Wacker 280-B | 8[b] | | brush |

[a] Solvent: ethyl acetate.
[b] Solvent: petroleum ether.

ization conditions probably leads to a block microstructure consisting of homo-TFEM and alternating TFEM-BVE sequences.

The application procedures of the coating materials on the stone specimens are summarized in Table III. The concentrations of the treating solutions have been chosen on the basis of the experience with similar acrylic or siloxane polymers, which are generally applied on stone substrates from 10 wt % or more diluted solutions. In the case of Acryloid B72™ and of its parent fluorinated copolymer TFEM/MA, the same concentrations (3 and 5 wt %) adopted in previous experiences[28,29] were employed.

### Polymer Uptake

Due to the low porosity of the Candoglia marble, a quite low amount of each copolymer solution penetrates into this stone, while the same copolymer solutions are easily absorbed into the highly porous structure of the calcarenite. When the coatings were applied by brush (Table III), the calcarenite specimens absorbed 4 to 10 times as much product as that absorbed by the marble specimens (Table IV). In the case of the products applied by capillarity, the amount of polymer absorbed was even higher, that is, from 40 to 100 times larger on the calcarenite. These differences are really important, and should be taken into account when evaluating the performances of the different protective coatings.

Indeed, the Candoglia marble, given the low amount of polymer that it can take up, is more difficult to protect than the calcarenite and, as it will be shown, does not always allow to clearly distinguish the variation in performance among different coating polymers. In addition, application by capillarity allows deeper and presumably more uniform penetration of the coating material into the porous stone structure than brush application, thus improving the effectiveness and duration of the imparted water repellency.

The presence of fluorine in the polymers and the length of the alkyl side chains do not appear to affect the polymer uptake by the stone, that is, the penetration of the copolymer solutions. Actually, the polymer absorption on a given stone type is mainly influenced by the application methodology.

**Table IV Amount of Coating Polymer Applied on the Specimen Surface**

| Coating Polymer[a] | Stone Specimen[b] | Applied Coating ($g/m^2$) | |
|---|---|---|---|
| | | Marble | Calcarenite |
| XFDM/LM-5 | A | 4.6 | 44.0 |
| | B | 5.3 | 54.9 |
| XFDM/LM-10 | A | 12.2 | 106.6 |
| | B | 13.9 | 144.7 |
| PLM-5 | A | 4.7 | 42.5 |
| | B | 5.1 | 59.3 |
| PLM-10 | A | 8.9 | 89.2 |
| | B | 11.7 | 102.4 |
| TFEM/MA-3 | A | 2.1 | 124.0 |
| | B | 4.6 | 273.5 |
| TFEM/MA-5 | A | 4.3 | 221.5 |
| | B | 7.1 | 396.0 |
| Acryloid B72-3 | A | 1.7 | 104.1 |
| | B | 2.5 | 204.4 |
| Acryloid B72-5 | A | 2.3 | 161.8 |
| | B | 3.1 | 299.4 |
| TFEM/BVE-5 | A | 8.4 | 34.0 |
| | B | 9.9 | 42.8 |
| TFEM/BVE-10 | A | 15.6 | 72.7 |
| | B | 19.2 | 91.6 |
| EM/BVE-5 | A | 11.5 | 31.0 |
| | B | 11.9 | 38.0 |
| EM/BVE-10 | A | 24.3 | 63.5 |
| | B | 29.8 | 82.9 |
| Wacker 280-C | A | 2.5 | 20.3 |
| | B | 3.5 | 28.0 |
| Wacker 280-B | A | 3.5 | 109.0 |
| | B | 6.3 | 224.5 |

[a] The number suffix identifies the concentration of the treating solution.
[b] $A = 5 \times 5$ (surface) $\times$ 1 (thickness) cm, $B = 5 \times 5 \times 2$ cm.

**Table V Contact Angle with Water of Treated Stone Surfaces**

| | Candoglia Marble | | | Noto Calcarenite | | |
|---|---|---|---|---|---|---|
| Treatment | $\theta$ | % n.d. | $\sigma$ | $\theta$ | % n.d. | $\sigma$ |
| Untreated | 42 | — | 2 | [a] | — | — |
| XFDM/LM-5 | 116 | — | 1 | 147 | 40 | 2 |
| XFDM/LM-10 | 117 | — | 2 | 141 | 13 | 4 |
| PLM-5 | 109 | — | 3 | 130 | 3 | 2 |
| PLM-10 | 115 | — | 2 | 132 | 2 | 2 |
| TFEM/MA-3 | 98 | — | 9 | 131 | 1 | 2 |
| TFEM/MA-5 | 94 | — | 5 | 130 | — | 3 |
| Acryloid B72-3 | 82 | — | 7 | 120 | — | 4 |
| Acryloid B72-5 | 77 | — | 3 | 118 | — | 4 |
| TFEM/BVE-5 | 91 | — | 3 | 132 | 1 | 3 |
| TFEM/BVE-10 | 92 | — | 3 | 129 | — | 3 |
| EM/BVE-5 | 92 | — | 2 | 126 | — | 4 |
| EM/BVE-10 | 89 | — | 1 | 109 | — | 7 |
| Wacker 280-C | 113 | — | 6 | 146 | 52 | 3 |
| Wacker 280-B | 115 | — | 5 | 143 | 46 | 3 |

$\theta$ = contact angle; % n.d. = percentage of drops not wetting the surface (rolled away after syringe deposition); $\sigma$ = standard deviation (30 measurements).

[a] The equilibrium contact angle of untreated calcarenite cannot be determined under the experimental condition adopted.

### Equilibrium Contact Angle with Water

Irrespective of the type of applied polymer, the measured contact angles $\theta$ with water are generally larger on the treated Noto calcarenite than on the treated Candoglia marble (Table V). However, because the equilibrium contact angle is affected by the extent of coverage of the stone surface by the thin polymer film, the surface roughness and the porosity of the treated stone (in Fig. 2 the different surface morphology of the marble treated with different copolymers is showen), these measurements always yield highly scattered data; therefore, the reported average $\theta$ values can only be considered for a comparative evaluation of the behavior of the different polymers applied to the same stone, rather than for a comparison of the effectiveness of a certain polymer on different stones.

On both stones the $\theta$ values obtained from the polymers XFDM/LM and PLM are the highest, and actually quite similar to those obtained from the siloxane treatment. The introduction of fluorine in these highly hydrophobic long side-chain polymers slightly improves their water repellence and, in the case of the Candoglia marble, this shows only at lower polymer load.

The presence of fluorine determines a much more significant increase of water repellence, both for the Candoglia marble and for the Noto stone, in the case of the short side-chain copolymers, as it is clearly seen by comparing the TFEM/MA copolymer with its unfluorinated analogous Acryloid B72. On the contrary, the TFEM/BVE and EM/BVE copolymers showed a quite similar behavior irrespective of the presence of fluorine, their water repellence being comparable with that of the TFEM/MA copolymer. In this latter case, the short fluorinated TFEM side chains are probably "masked" by the longer *n*-butyl side chains, and do not increase the effectiveness of the hydrophobic shield provided by the EM/BVE copolymer.

### Water Absorption by Capillarity

The untreated 2 cm-thick stone specimens were quickly saturated by water, reaching a plateau of 30–50 g/m$^2$ within the first 3–6 h (100–150 s$^{1/2}$) for the marble and as much as of 4500–5000 g/m$^2$ within the first 20–40 h for the calcarenite. As it is shown in Figures 3–8, all treatments led to a more or less pronounced reduction in absorption, at least at short times. The capillarity curves in Figures 3–8 are reported as "% reduction of absorbed water"—instead of the more frequently used "amount of absorbed water"—against the

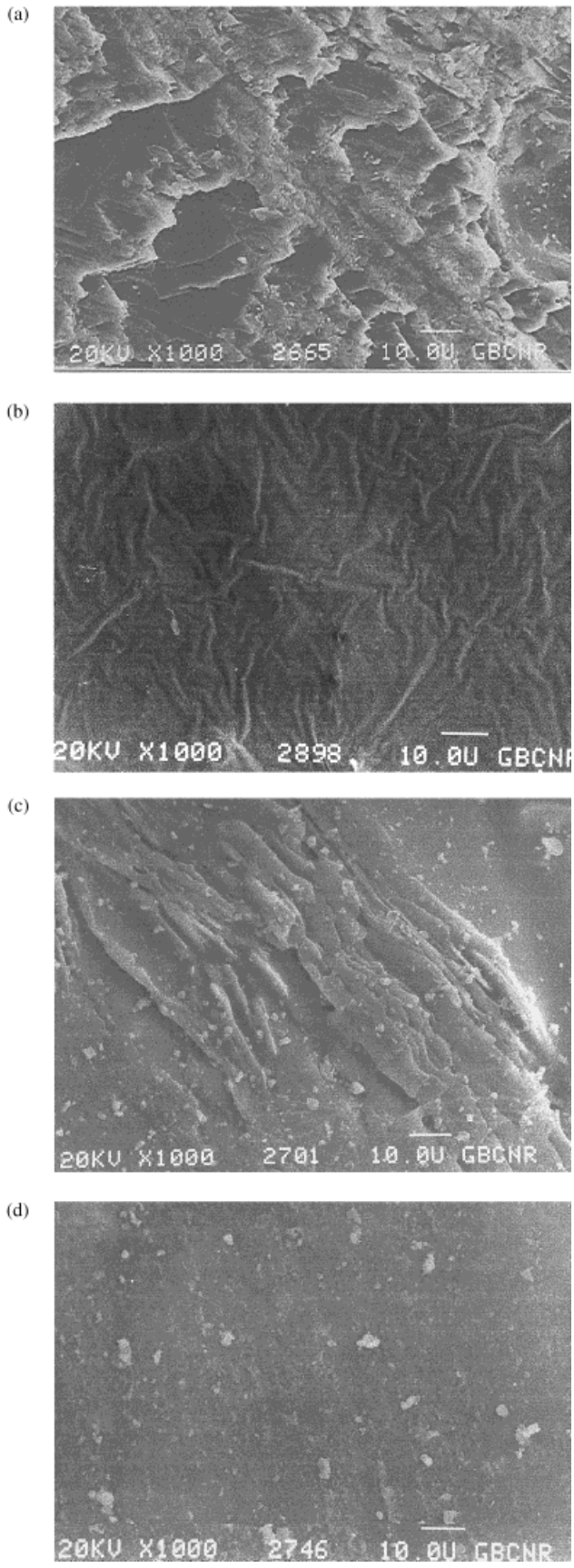


square root of time ($s^{1/2}$); this allows direct comparison of the efficacy of the various coating polymers, independently from the amount of water absorbed by each untreated stone specimen (which can be quite variable), by comparing the % reduction of water absorption achieved upon coating each specific stone specimen.

### Candoglia Marble

All fluorinated polymers determine a higher reduction of water absorption than their unfluorinated analogues, as it is shown in Figures 3–5; in the case of TFEM/BVE and XFDM/LM such improvement is particularly apparent at shorter times (less than 24 h—300 $s^{1/2}$). TFEM/BVE is the most effective in maintaining a moderate long-term water repellency which, on the contrary, is lost on the EM/BVE-coated stone. On the other side, XFDM/LM is the most effective at short contact times, cutting off about 90% of the water absorption after 6 h—150 $s^{1/2}$, that is, even more than the quite effective PLM and with a performance comparable to that of the Wacker siloxane (Fig. 3). However, the protection efficacy of these latter long-side chain, low-$T_g$ copolymers drops considerably, and at longer times it is almost completely lost. The short side-chain TFEM/MA copolymer, although clearly less effective than the Wacker siloxane (Fig. 4) and slightly less than the TFEM/BVE copolymer, performs better than XFDM/LM at times exceeding 48 h (400 $s^{1/2}$), when its protection efficacy reaches a plateau at about 20% water absorption reduction.

This apparently strange behavior can be understood in terms of local reorganization of the coating material at the polymer–water interface, i.e., as a result of aging in the presence of condensed water. In these conditions the long fluoroalkyl side chains of the low-$T_g$ XFDM/LM copolymer, which are presumably "clustered" to form microphase-segregated domains at the polymer–air interface, can easily undergo thermodynamically driven conformational rearrangement to minimize their exposure to water. As the consequence, the coating surface becomes enriched in polar ester groups, thereby enhancing its wetta-

**Figure 2** SEM micrographs (1000×) of the Candoglia marble surface before (a) and after application of the flourinated copolymers XFDM/LM (b), TFEM/MA (c), and TFEM/BVE (d).

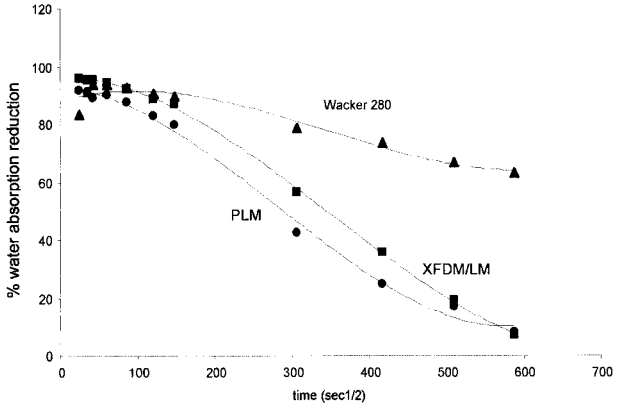


**Figure 3** Water capillary absorption on the marble: % reduction upon coating with XFDM/LMA and poly-LMA, and for comparison, with the Wacker silicone.

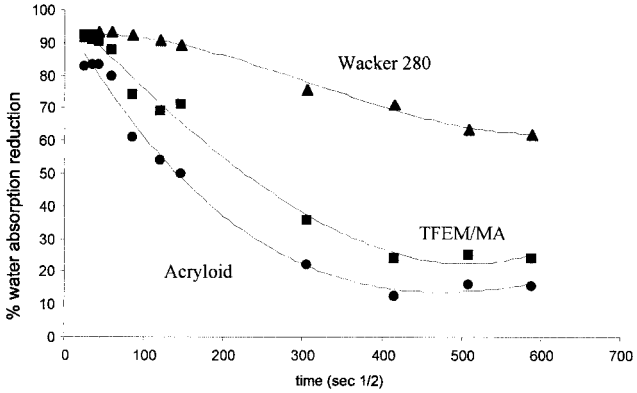


**Figure 4** Water capillary absorption on the marble: % reduction upon coating with TFEM/MA and Paraloid B72, and for comparison, with the Wacker silicone.

bility and allowing easier diffusion of water either through the bulk of the polymer (containing a relatively low mol fraction of fluorinated counits) or by capillary absorption inside the polymer-coated stone pores. In the case of the TFEM/MA copolymer, containing a much higher mol fraction of fluorinated units, the $CF_3$ groups are more likely to be homogeneously distributed in the bulk of the polymer with little enrichment at the polymer–air interface; therefore, the good but not outstanding performance of the coating at short contact times is balanced by its fair and long-lasting water repellence properties, which are only overrun by the highly hydrophobic TFEM/BVE.

The fluorinated vinyl ether copolymer TFEM/BVE indeed presents a resistance to water penetration that is unexpectedly higher than that of the fully acrylic TFEM/MA, at least if one takes the water contact angle (Table 5) as a first indication of the coating water repellency. The effect of the introduction of fluorine in the vinyl ether copolymer can be best observed at longer times (Fig. 5), when only the fluorinated coating preserves a certain water repellency, and to a degree that makes it the best performer among all the acrylic copolymers studied.

In general, the concentration of the treating solution does not affect the coating performance. It must be noted, however, that although these polymers perform relatively well, the appearance of the coated marble surface is in some cases very poor, due to darkening (see the Color Changes Evaluation section), undesired gloss and, particularly for the long side-chain polymers, tackiness caused by the insufficient penetration of the polymer into the compact crystalline matrix of the marble.

## Calcarenite of Noto

The higher polymer uptake allowed by this porous stone, as well as the higher porosity of the untreated stone, determine a much sharper decrease of the water absorption on the coated specimens if compared with that observed for the treated marble. The water absorption curves of Figures 6–9 allow one to clearly distinguish among the performances of the different coating materials. Again, all fluorinated polymers determine a higher reduction of water absorption (which is initially comparable with that of the Wacker siloxane) than their unfluorinated analogues, particularly after the first 6 h (150 $s^{1/2}$); however, on the Noto stone such a difference is much more striking than on the marble.

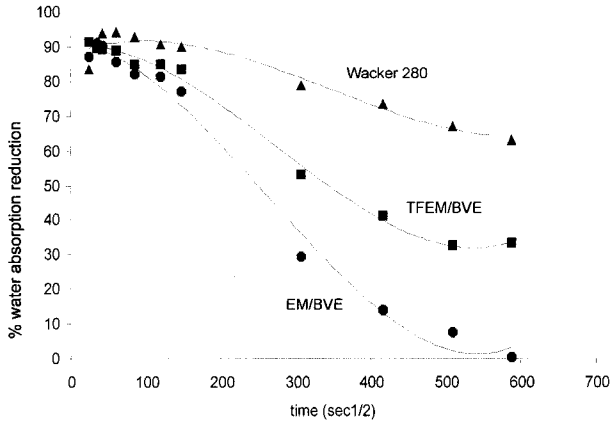


**Figure 5** Water capillary absorption on the marble: % reduction upon coating with TFEM/BVE and EM/BVE, and for comparison, with the Wacker silicone.

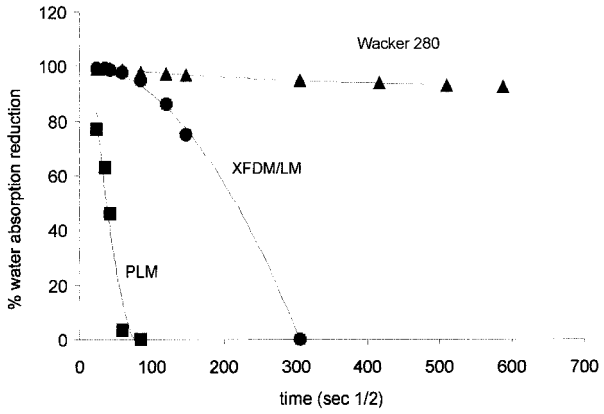


**Figure 6** Water capillary absorption on the calcarenite: % reduction upon coating with XFDM/LMA and poly-LMA, and for comparison, with the Wacker silicone.

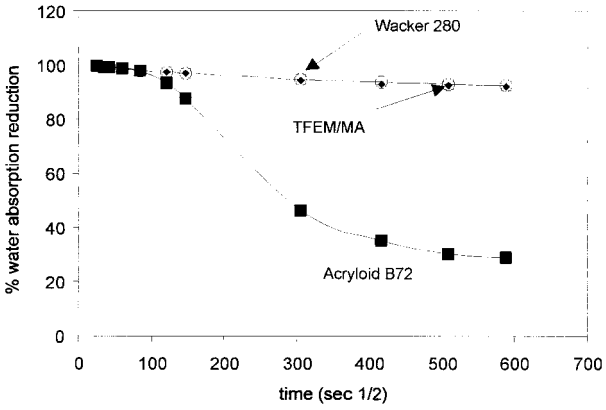


**Figure 7** Water capillary aborption on the calcarenite: % reduction upon coating with TFEM/MA and Paraloid B72, and for comparison, with the Wacker silicone.

Among the three fluorinated copolymers, XFDM/LM is the worst performer, because it starts losing efficacy after less than 6 h (150 $s^{1/2}$) and becomes completely ineffective after 24 h (Fig. 6). This is, however, a fair result if compared with the behavior of PLM, at least when using the highest concentration of treating solution; both coatings applied from the 5% solutions are indeed almost ineffective. Lack of penetration into the stone can also account for the poor performance of this material, despite the fact that the amount of product applied on the calcarenite is about 10 times greater than that applied on marble.

The performances of TFEM/MA, TFEM/BVE, and EM/BVE are, on the other hand, very interesting, as they are compared to that of the reference siloxane product (Figs. 7 and 8). TFEM/MA displays its improved behavior, with respect to Acryloid B72, after the first 6 h, when the fluorinated coating preserves its protection effect while a progressive recover of the water permeability is displayed by the unfluorinated one (Fig. 7). The difference between the fluorinated and unfluorinated polymer is less evident in the case of the vinyl ether copolymers (Fig. 8), simply because both materials perform extremely well up to 72 h (500 $s^{1/2}$), when the unfluorinated coating starts losing efficacy. When comparing the two TFEM copolymers, one can observe that replacement of the methyl acrylate with the *n*-butyl vinyl ether unit determines a decrease of the $T_g$; this, in addition to the lower polarity of the vinyl ether unit and, therefore, to its reduced affinity for water, affects positively the coating performance. This is best seen on the marble substrate (Fig. 9), while on the calcarenite (Fig. 10) both TFEM/BVE and TFEM/MA have a protection efficiency comparable with that of the silicone (Figs. 7 and 8).

## Water Vapor Permeability

The results of the water vapor permeability measurements are collected in Table VI. The vapor permeability of the marble specimens, already very low for the untreated stone, is clearly reduced by the application of the fluorinated copolymers. The difference between the TFEM/MA and the Acryloid B72 coatings is quite evident: the introduction of fluorine in the macromolecule determines a sharp decrease of the permeability, independent from the

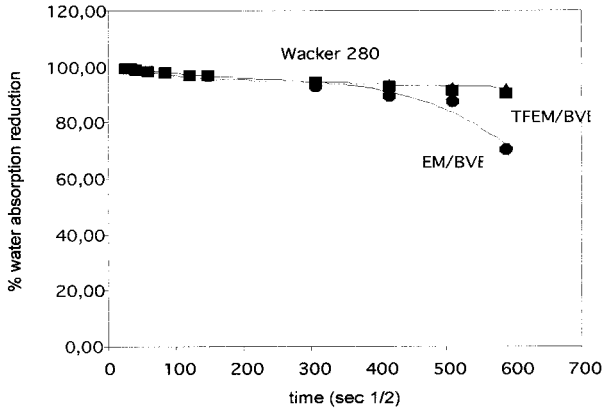


**Figure 8** Water capillary absorption on the calcarenite: % reduction upon coating with TFEM/BVE and EM/BVE, and for comparison, with the Wacker silicone.

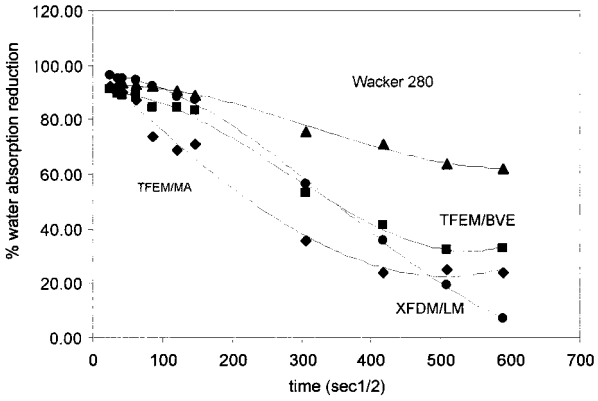


**Figure 9** Water capillary absorption on the marble: % reduction upon coating with the flourinated copolymers XFDM/LM, TFEM/MA, and TFEM/BVE, compared with the Wacker silicone.

starting solution concentration, that is from the amount of applied product. However, a very pronounced reduction of permeability is also obtained upon treatment of the specimens with the highly water-repellent Wacker siloxane. The situation is very different in the case of the highly porous calcarenite. The reduction of the permeability is well less worrying and quite similar, for all copolymers, to that obtained by treating the specimen with the Wacker 280 product. The introduction of fluorine does not produce a pronounced reduction in the permeability of the coated surfaces, while, in some cases, a reduction can be observed if one compares the same copolymer at different concentration of the treating solution—that is, at different polymer uptake.

As a general rule, the data here reported suggest that the introduction of fluorine determines a certain reduction of the water vapor permeability; however, this kind of property is strongly affected by the treating methodology (e.g., by capillarity or by brush) and by the porous structure of the stone. A detailed study of the influence, on the water transport properties, of the polymer amount and distribution on the stone surface and within its pores, however, goes beyond the scope of the present work.

## Color Changes Evaluation

When analyzing the color changes in the L*a*b* system (Table VII), the most significant parameter, from the statistical point of view, is the lightness difference ΔL*; in this respect, all the treatments produced a darkening of the specimen, as L* values are always increasing. This change is more pronounced in the case of the calcarenite; this is not unexpected, given the much larger amount of polymer absorbed on this stone per unit area, and it shows particularly at higher treating solution concentrations. In addition, the parameters b* (indicating a displacement of chromaticity from blue to yellow), a* (displacement of the chromaticity towards the red), and the excitation purity *P* (the difference in the color saturation calculated by the CIE system) are also affected by a statistically significant change after treatment of the Calcarenite. Larger variations are observed in the case of the couple of polymers XFDM/LM and PLM-coated specimens, while the siloxane product produces the slightest effect. The color changes on the marble specimens after treatment, although statistically significant, are less important. The darkening, indicated by the negative ΔL* values, is similar for all treatments and generally quite low; a comparatively larger variation with respect to the calcarenite is induced by treatment with the siloxane product. The study of the colour variations induced by the introduction of fluorine in the macromolecules allowed to conclude that no significant change of L*, a*, and b* could be associated to this factor in the case of the marble. On the contrary, the introduction of fluorine produces a significant color modification of these parameters in the case of the calcarenite. In particular, the treatment with XFDM/LM and TFEM/BVE produces a clearing up of the specimens, if the L* values are compared with those of the specimens treated with

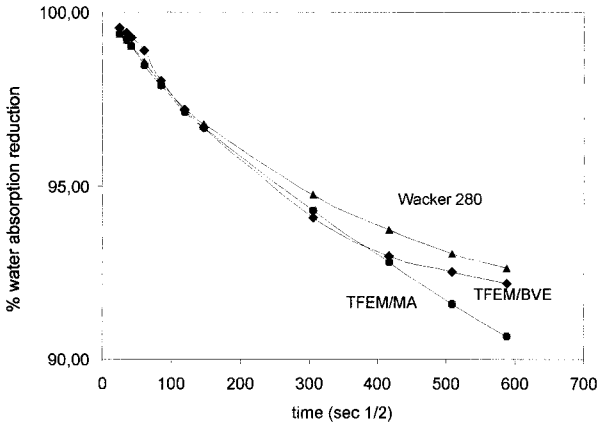


**Figure 10** Water capillary absorption on the calcarenite: % reduction upon coating with the fluorinated copolymers TFEM/MA and TFEM/BVE, compared with the Wacker silicone.

**Table VI Water Vapor Permeability Reduction upon Coating of Stone Specimens; Determined as Net Flux of Water Vapor over a 24-h Period**

| | Water Vapor Permeability ($g/m^2 \cdot 24$ h) | | % Reduction after Treatment | |
|---|---|---|---|---|
| Treatment | Untreated Marble | Untreated Calcarenite | Candoglia Marble | Noto Calcarenite |
| XFDM/LM-5 | 14.9 | 329.7 | 77.3 | 24.6 |
| XFDM/LM-10 | 12.2 | 320.2 | 75.4 | 51.1 |
| PLM-5 | 14.2 | 333.4 | 61.8 | 22.8 |
| PLM LM-10 | 13.1 | 303.0 | 75.8 | 26.7 |
| TFEM/MA-3 | 12.4 | 299.2 | 80.7 | 24.7 |
| TFEM/MA-5 | 13.4 | 304.9 | 78.0 | 39.4 |
| Acryloid B72-3 | 14.2 | 292.7 | 57.7 | 35.2 |
| Acryloid B72-5 | 13.0 | 313.0 | 46.9 | 39.4 |
| TFEM/BVE-5 | 17.9 | 301.1 | 57.0 | 15.5 |
| TFEM/BVE-10 | 16.1 | 313.8 | 70.8 | 27.7 |
| EM/BVE-5 | 14.2 | 255.6 | 53.1 | 10.4 |
| EM/BVE-10 | 13.1 | 301.7 | 43.0 | 33.0 |
| Wacker 280-C | 7.9 | 313.9 | 77.2 | 35.4 |
| Wacker 280-B | 5.5 | 288.8 | 69.1 | 12.8 |

the homologues unfluorinated polymers (PLM and EM/BVE).

## CONCLUSIONS

The work described here was aimed at correlating, in a direct way, polymer structure to stone protection performance. Even if many aspects connected to the complexity of the stone substrate and polymer application procedure may still play a significant role, the present approach should offer a useful feedback to polymer chemists, helping to design improved protective materials.

As expected, side-chain fluorination improves the coating efficacy of these acrylic and acrylic–

**Table VII Stone Specimen Surface Color Variation after Treatment with the Coating Polymers[a]**

| | Candoglia Marble | | | | Noto Calcarenite | | | |
|---|---|---|---|---|---|---|---|---|
| Treatment | $\Delta L^*$ | $\Delta a^*$ | $\Delta b^*$ | $\Delta P\%$ | $\Delta L^*$ | $\Delta a^*$ | $\Delta b^*$ | $\Delta P\%$ |
| XFDM/LM-5 | −1.29 | 0.04[a] | 0.56 | 0.68 | −6.76 | 2.31 | 7.32 | 10.70 |
| XFDM/LM-10 | −2.08 | −0.04[a] | 0.75 | 0.92 | −8.95 | 2.50 | 7.15 | 11.34 |
| PLM-5 | −1.98 | −0.01[a] | 0.61 | 0.76 | −7.65 | 2.49 | 7.84 | 11.57 |
| PLM LM-10 | −2.36 | 0.00[a] | 0.64 | 0.47 | −10.53 | 2.88 | 7.74 | 12.49 |
| TFEM/MA-3 | −1.85 | 0.11 | 0.69 | 0.74 | −7.42 | 1.76 | 5.10 | 7.89 |
| TFEM/MA-5 | −2.14 | −0.02[a] | 0.46 | 0.56 | −8.63 | 2.00 | 5.28 | 8.67 |
| Acryloid B72-3 | −1.48 | −0.01[a] | 0.30 | 0.35 | −7.48 | 1.91 | 5.40 | 8.66 |
| Acryloid B72-5 | −1.87 | 0.02[a] | 0.36 | 0.38 | −8.56 | 2.11 | 5.62 | 9.18 |
| TFEM/BVE-5 | −2.61 | 0.04[a] | 0.68 | 0.88 | −5.06 | 1.30 | 4.61 | 6.76 |
| TFEM/BVE-10 | −2.44 | 0.04[a] | 0.27 | 0.30 | −6.83 | 1.66 | 5.01 | 7.53 |
| EM/BVE-5 | −2.11 | 0.08 | 0.64 | 0.80 | −5.86 | 1.41 | 5.04 | 7.50 |
| EM/BVE-10 | −2.52 | 0.11 | 0.46 | 0.40 | −7.74 | 1.91 | 5.88 | 9.37 |
| Wacker 280-C | −3.07 | 0.00[a] | 0.52 | 0.69 | −2.60 | 0.55 | 1.79 | 2.73 |
| Wacker 280-B | −2.89 | −0.01[a] | 0.59 | 0.76 | −1.72 | 0.30 | 1.06 | 1.61 |

[a] Values to be considered negligible (statistically not significant due to large scattering of experimental data).

vinyl ether copolymers, although their performance is never better than that of the alkylalkoxy siloxane product. As it has already discussed in the introduction, the latter material has a quite different mechanism of interaction with the stone, creating an irreversible network with it.

The results of the capillarity water absorption measurements have clearly shown that the instantaneous water repellence of a coating material, as indicated by contact angle data, is a somewhat misleading information if a durable protection in wet conditions is required. In particular, the outstanding protection efficacy of the long side-chain XFDM copolymer appears to be extremely short lasting, presumably due to local reorganization of the fluoroalkyl groups at the polymer–water interface as a result of aging in the presence of condensed water. In the absence of an effective mechanism of "reversible crosslinking," capable of granting the permanence of a highly fluorinated polymer–water interface, the improved bulk impermeability provided by the short side-chain TFEM copolymers appears to better match the requirements of a good short-term and fair long-term protection efficacy of these reversible coating materials. Among these latter copolymers, the TFEM/BVE has shown the best coating efficacy in terms of reduced water absorption with modest reduction of vapor permeability and acceptable chromatic properties. However, preliminary results indicate an insufficient photostability of this material, suggesting that the tertiary carbon atom with a labile CH bond on the vinyl ether unit determines a much higher tendency towards photodegradation compared to the same bond in the copolymers with the MA unit. Further studies are being carried out to investigate how the overall fluorine content and distribution along the macromolecule influences the coating properties and the polymer photostability, with a particular attention devoted to alternated copolymer structures. Finally, a thorough understanding of the photodegradation behavior of coating materials on porous substrates needs to be addressed, because quite different photodegradation pathways could arise from the polymer–substrate interaction.

The long side-chain XFDM copolymer induces a pronounced darkening of the porous stone substrate, while chromatic changes are almost negligible on the marble. On this last substrate the low $T_g$ copolymers give rise to an undesired tackiness phenomena. The darkening of the calcarenite is, nevertheless, a general problem when treating this substrate with acrylic polymers, so a compromise should be accepted between good performances and color variations.

Financial support from the C.N.R. "Safeguard of Cultural Heritage" Target Project (http://soi.cnr.it/~tminfo/culturalheritage/) is gratefully acknowledged.

## REFERENCES

1. Canelas, D. A.; De Simone, J. M. Adv Polym Sci 1997, 133, 104.
2. (a) Arias, E. M.; Putnam, M. D.; Boss, P. A.; Boss, R. D.; Anderson, A. A.; George, R. D. ACS Polym Prepr 1997, 38, 512; (b) Altmann, K. L.; Merwin, L. H.; George, R. D. ACS Polym Prepr 1997, 38, 786.
3. Grainger, D. W.; Wang, W.; Castner, D. Polym Mater Sci Eng 1997, 77, 587.
4. Garbassi, F.; Morra, M.; Occhiello, E. Polymer Surfaces; John Wiley: New York, 1994, p. 327.
5. Piacenti, F. Sci Total Environ 1994, 143, 113.
6. Lazzarini, L.; Laurenzi Tabasso, M. Il restauro della Pietra; CEDAM: Padova, Italy, 1986, p. 216.
7. Amoroso, G. G.; Fassina, V. Stone Decay and Conservation; Elsevier: Amsterdam, The Netherlands, 1983.
8. Winkler, E. M. Stone: Properties, Durability in Man's Environment; Springer-Verlag: Wien, 1975.
9. Charola, A. E.; Delgado Rodrigues, J. Sci Technol Cultural Heritage 1996, 5, 111.
10. Normal Protocol 20/85. Conservation Works: Planning, Execution and Preventive Evaluation; ICR-CNR: Rome, Italy, 1985.
11. Puterman, M.; Jansen, B.; Kober, H. J Appl Polym Sci 1996, 59, 1237.
12. (a) Thomas, R. R.; Anton, D. R.; Graham, W. F.; Darmon, M. J.; Sauer, B. B.; Stika, K. M.; Schwartzfager, D. G. Macromolecules 1997, 30, 2883; (b) Krupers, M.; Möller, M. Macromol Chem Phys 1997, 198, 2163; (c) Park, I. J.; Lee, S.-B.; Choi, C. K. Polymer 1997, 38, 2523.
13. (a) Charola, A. E.; Laurenzi Tabasso, M.; Santamaria, U. Proceedings of the 5th International Congress on Deterioration and Conservation of Stone, Lausanne, 1985, p. 739; (b) Biscontin, G.; Zendri, E.; Schionato, A. Mater Struct 1991, 1, 95; (c) Villegas, R.; Valle, J. F. Proceedings of the 7th International Congress on the Deterioration and Conservation of Stone, Lisbon, 1992, p. 1253.
14. (a) Botteghi, C.; Matteoli, U.; Paganelli, S.; Arbizzani, R.; Ciardelli, F.; Aglietto, M.; Taburoni, E.; Fassina, V. Sci Technol Cultural Heritage 1992, 1, 111; (b) Matteoli, U.; Aglietto, M.; Fassina, V.; Botteghi, C.; Passaglia, E.; Ciardelli, F. Preprints of the ICCROM International Colloquium on Methods of evaluating Products for the Conservation of

Porous Building Materials in Monuments, Rome, 1995, p. 373; (c) Ciardelli, F.; Aglietto, M.; Montagnini di Mirabello, L.; Passaglia, E.; Giancristoforo, S.; Castelvetro, V.; Ruggeri, G. Prog Organ Coatings 1998, 32, 43.
15. Ciardelli, F.; Aglietto, M.; Montagnini di Mirabello, L.; Passaglia, E.; Ruggeri, G. Paints Varnishes 1996, 72, 21.
16. Castelvetro, V.; Aglietto, M.; Montagnini di Mirabello, L.; Toniolo, L.; Peruzzi, R.; Chiantore, O. Surface Coatings Int 1998, 81, 551.
17. Aglietto, M.; Passaglia, E.; Taburoni, E.; Ciardelli, F.; Botteghi, C.; Matteoli, U.; Paganelli, S.; Arbizzani, R.; Fassina, V. ICOM Committee for Conservation, Vol. II, 1993, p. 553.
18. Normal Protocol 33/89 Contact Angle Determinations; ICR-CNR: Roma, Italy, 1991.
19. Normal Protocol 11/85 Water Absorption by Capillarity. Capillarity Absorption Coefficient; ICR-CNR: Roma, Italy, 1986.
20. (a) Vos, B. H. Studies in Conservation 1971, 16, 129; (b) Rosa, R. N. In Proceedings of EC Workshop Degradation and Conservation of Granitic Rocks; Vincente, M. A.; Delgado Rodriguez, J.; Acevedo, J. Santiago Comp 1994, p. 255.
21. Normal Protocol 21/85 Water Vapour Permeability; ICR-CNR: Roma, Italy, 1986.
22. Normal Protocol 43/93 Colour determinations of opaque surfaces; ICR-CNR: Roma, Italy, 1994.
23. Hunter, R. S. The Measurement of Appearance; John Wiley: New York, 1975.
24. Johnston, R. M. In Pigment Handbook; Patton, T. C.; John Wiley & Sons: New York, 1973, p. 229, vol. III.
25. Wright, W. D. The Measurement of Color; Adam Hilger: London, 1969, 4th ed.
26. Chiantore, O.; Lazzari, M. Int J Polym Anal Charact 1996, 2, 395.
27. De Witte, E.; Verheyen, A.; De Bruyn, R.; Pien, A. Sci Technol Cultural Heritage 1993, 2, 173.
28. Aldi, A.; Alessandrini, G.; Casarino, A.; Pedemonte, E.; Peruzzi, R. Preprints of the ICCROM International Colloquium on Methods of evaluating Products for the Conservation of Porous Building Materials in Monuments, Rome, Italy, 1995, p. 285.
29. Kumar, R.; Ginell, W. S. J Am Instit Conservat 1997, 36, 143.